Research Article | Vol. 27, No. 7 | 1 Apr 2019 | OPTICS EXPRESS 9987

Optics EXPRESS

"Mixed" Tm:Ca(Gd,Lu)AlO_4 — a novel crystal for tunable and mode-locked 2 µm lasers

ZHONGBEN PAN,[1,2] PAVEL LOIKO,[3] JOSEP MARIA SERRES,[4] ESROM KIFLE,[4] HUALEI YUAN,[1] XIAOJUN DAI,[1] HUAQIANG CAI,[1] YICHENG WANG,[2] YONGGUANG ZHAO,[2,5] MAGDALENA AGUILÓ,[4] FRANCESC DÍAZ,[4] UWE GRIEBNER,[2] VALENTIN PETROV,[2] AND XAVIER MATEOS[4,*]

[1]*Institute of Chemical Materials, China Academy of Engineering Physics, Mianyang 621900, China*
[2]*Max Born Institute for Nonlinear Optics and Short Pulse Spectroscopy, Max-Born-Str. 2a, D-12489 Berlin, Germany*
[3]*ITMO University, 49 Kronverkskiy Pr., 197101 Saint-Petersburg, Russia*
[4]*Universitat Rovira i Virgili, Depart. Quimica Fisica i Inorganica, FiCMA-FiCNA-EMaS, Campus Sescelades, E-43007 Tarragona, Spain*
[5]*Jiangsu Key Laboratory of Advanced Laser Materials and Devices, Jiangsu Normal University, 221116 Xuzhou, China*
**xavier.mateos@urv.cat*

Abstract: We report on the crystal growth, spectroscopy characterization and first laser operation of a new tetragonal disordered "mixed" calcium aluminate crystal, Tm:Ca(Gd,Lu)AlO_4. The introduction of Lu^{3+} leads to an additional inhomogeneous broadening of Tm^{3+} absorption and emission spectra compared to the well-known Tm:$CaGdAlO_4$. The maximum stimulated-emission cross-section for the $^3F_4 \rightarrow {}^3H_6$ Tm^{3+} transition is 0.91×10^{-20} cm^2 at 1813 nm for σ-polarization, and the emission bandwidth is more than 200 nm. A continuous-wave diode-pumped Tm:Ca(Gd,Lu)AlO_4 laser generates 1.82 W at 1945 nm with a slope efficiency of 29%. Under Ti:Sapphire laser pumping, a continuous tuning of the laser wavelength from 1836 to 2083 nm (tuning range: 247 nm) is demonstrated. The Tm:Ca(Gd,Lu)AlO_4 crystal is promising for tunable/femtosecond lasers at ~2 µm.

1. Introduction

Tetragonal (space group *I*4/*mmm*) calcium rare-earth aluminates $CaLnAlO_4$ (where Ln = Gd or Y, abbreviated as CALGO and CALYO, respectively) are well-known disordered laser crystal hosts for Yb^{3+}-doping [1,2]. They feature high thermal conductivity (~6.5 W/mK for $CaGdAlO_4$) with a weak concentration-dependence and weak and positive thermal lensing originating from negative thermo-optic coefficients, d*n*/d*T* [3]. The structural disorder originates from a random distribution of Ca^{2+} and Ln^{3+} cations over a single type of sites (C_{4v}) [2]. This leads to a significant inhomogeneous broadening of absorption and emission bands making these crystals attractive for sub-100 fs mode-locked (ML) lasers at ~1 µm in the case of Yb^{3+} doping [4,5]. Good thermo-mechanical properties of $CaLnAlO_4$-type crystals enable power scaling of Yb^{3+} oscillators [6].

Considering the success of Yb:$CaLnAlO_4$ crystals, the research interest turned to their doping with Thulium (Tm^{3+}) ions. The latter are known for their eye-safe emission in the spectral range of ~2 µm ($^3F_4 \rightarrow {}^3H_6$ transition) [7]. The Tm^{3+} ions show efficient absorption at ~0.8 µm (to the $^3H_4$ state), e.g., emission from Ti:Sapphire lasers or commercial powerful AlGaAs laser diodes. Efficient cross-relaxation for adjacent Tm^{3+} ions, $^3H_4 + {}^3H_6 \rightarrow {}^3F_4 + {}^3F_4$, may raise the pump quantum efficiency up to 2 leading to high laser efficiency and reduced heat loading [8]. Due to the typically large Stark splitting of the ground-state ($^3H_6$), the ~2 µm

#357666 https://doi.org/10.1364/OE.27.009987
Journal © 2019 Received 18 Jan 2019; revised 16 Mar 2019; accepted 17 Mar 2019; published 26 Mar 2019

Optics EXPRESS

Tm^{3+} emission band is broad opening the possibility of broadband wavelength tuning of the laser emission and ML laser operation.

In 1990s, Tm:$CaYAlO_4$ crystals were initially studied [9,10]. In the recent years, Tm^{3+}-doped $CaLnAlO_4$ crystals were revisited regarding their growth, spectroscopic properties [11–13] and continuous-wave (CW) laser emission at ~2 μm [12,14]. In [14], a diode-pumped Tm:$CaYAlO_4$ laser generated a maximum output power of 7.62 W at 1945 nm with a slope efficiency of 50.9% (*vs*. the absorbed pump power). Passive Q-switching of such lasers by Cr^{2+}:ZnSe saturable absorbers has been reported [15]. Recently, an in-band pumping scheme (at ~1.7 μm, directly to the upper laser level, $^3F_4$) was explored for Tm:$CaYAlO_4$ leading to the generation of 6.8 W at 1968 nm with a slope efficiency of 52% (*vs*. the incident pump power) [16].

Regarding ML Tm:$CaLnAlO_4$ lasers, a remarkable result is the generation of femtosecond pulses (650 fs) from a Tm:$CaGdAlO_4$ laser ML by a GaSb-based SEmiconductor Saturable Absorber Mirror (SESAM) [17]. The central wavelength of the laser spectrum was at 2021 nm with a full width at half maximum (FWHM) of 9.2 nm. Such a long laser wavelength (for Tm^{3+}-doped crystals) was because a special "bandpass" output coupler was employed and the laser was constrained to oscillate above 2 μm. This had a key effect for achieving fs pulses. In [18], a SESAM ML Tm:$CaYAlO_4$ laser operating at 1961 nm generated pulses with a duration as long as 35.3 ps.

Note that for most of the laser materials doped with Tm^{3+}, the center of the $^3F_4 \rightarrow {}^3H_6$ emission band is located slightly below 2 μm. This is unfavorable for ML because the laser emission spectrally overlaps with the atmosphere water vapor absorption bands preventing fs mode-locking. One way to solve this problem is to use special wavelength-selective cavity mirrors as described above to constrain the laser to operate at >2 μm (the corresponding part of the gain spectrum is related to the electron-phonon (vibronic) interaction [19]). Another option is to use a very limited number of host materials ensuring large Stark splitting of the $^3H_6$ Tm^{3+} ground-state (e.g., cubic sesquioxides [20]). Recently, a new monoclinic Tm:$MgWO_4$ crystal generating laser emission above 2 μm enabled the generation of 86 fs pulses at 2017 nm [21]. An alternative is to provide an additional inhomogeneous broadening of Tm^{3+} emission by structure disorder or compositional disorder (in a "mixed" crystal) of the host material affecting the crystal field. Recently, various Tm^{3+}-doped crystals and ceramics with structure or compositional disorder were studied for fs ML lasers at ~2 μm [22,23].

In the present work, we aimed to grow and study the spectroscopic and laser properties of a novel calcium aluminate crystal, Tm:Ca(Gd,Lu)AlO_4. The addition of optically passive Lu^{3+} ions is expected to provide additional compositional disorder leading to further spectral broadening which is attractive for fs pulse generation in ML lasers. Note that the existence of the $CaLuAlO_4$ crystal has never been reported so far. The growth and spectroscopy of an Yb:Ca(Gd,Lu)AlO_4 crystal was recently studied [24].

2. Crystal growth and structure

The Tm:Ca(Gd,Lu)AlO_4 crystal melts congruently and thus it was grown by the conventional Czochralski (Cz) method using an Ar atmosphere in an Ir crucible. An automatic system was used to control the boule diameter. The polycrystalline samples were obtained by solid-state reaction from a mixture of the starting materials, 4N-pure $CaCO_3$, Gd_2O_3, Lu_2O_3, Al_2O_3 and 5N-pure Tm_2O_3. They were placed in an Ir crucible and melted by an intermediate-frequency heater. A [001]-oriented $CaGdAlO_4$ seed was used, the pulling rate was 0.5 mm/h and the rotation speed was 8 rpm. After the growth was completed, the crystal was cooled down to room temperature at a stepping rate of 15-25 K/h. A crack-free large-volume as-grown boule, Fig. 1(a), had a yellow coloration, attributed to interstitial oxygen atoms. The coloration was removed to a great extent by annealing at 950 °C for 24 h under N_2 atmosphere with 5% H_2.

The concentration of doping ions was measured by Inductively Coupled Plasma Mass Spectrometry (ICP-MS) to be 3.5 at.% Tm^{3+} and 5.2 at.% Lu^{3+}. The segregation coefficients

Optics EXPRESS

$K = N_{crystal}/N_{melt}$ for these ions are 0.70 and 0.52, respectively. The stoichiometric crystal formula is $CaGd_{0.913}Lu_{0.052}Tm_{0.035}AlO_4$. The Tm^{3+} ion concentration is $4.31 \times 10^{20}/cm^3$ (crystal density: $\rho = 6.01$ g/cm^3).

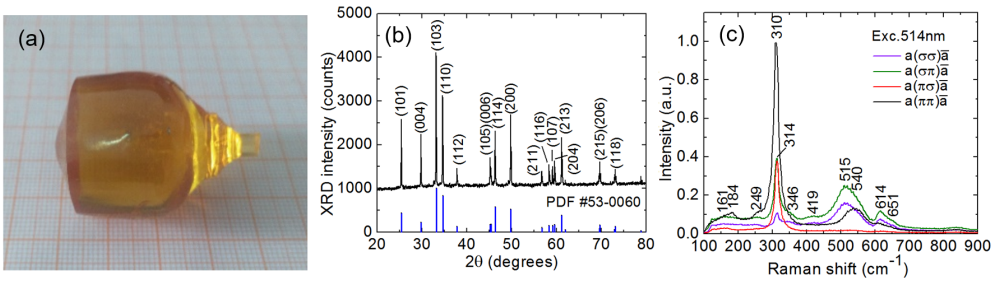

Fig. 1. (a) Photograph of the as-grown Tm:Ca(Gd,Lu)AlO_4; (b) X-ray powder diffraction (XRD) pattern (in *black*), *numbers* denote the Miller's indices (*hkl*), standard XRD pattern of $CaGdAlO_4$ is shown for comparison (in *blue*); (c) polarized Raman spectra of an ***a***-cut crystal, *a*(*xy*)*a* are the Porto's notations, *numbers* denote the peak Raman frequencies in cm^{-1}, λ_{exc} = 514 nm.

In $CaGdAlO_4$, the Ca^{2+} and Gd^{3+} cations (ionic radii R_{Ca} = 1.180 Å, R_{Gd} = 1.107 Å) statistically occupy the same type of site (Wyckoff symbol: 4*e*, site symmetry: C_{4v}, coordination number: IX). Tm^{3+} (R_{Tm} = 1.052 Å) and Lu^{3+} (R_{Lu} = 1.032 Å) cations are entering these sites. The local disorder results from the second coordination sphere of Tm^{3+} ions constituted by $Gd^{3+}|Lu^{3+}$ and Ca^{2+} ones, namely the charge difference of these ions and the different cation-cation distances. Note that doping of Ca(Gd,Lu)AlO_4 by both Tm^{3+} and Lu^{3+} ions is expected to affect the crystal field because of the closeness of their ionic radii. In this way, one can argue that solely high Tm^{3+} doping can produce a similar effect to Tm^{3+}, Lu^{3+} codoping. In the latter case, first, better crystal quality is achieved. Moreover, one avoids the unwanted energy-transfer upconverison related to very high Tm^{3+} concentration.

The structure and phase purity of Tm:Ca(Gd,Lu)AlO_4 were determined by X-ray powder diffraction (XRD), Fig. 1(b). The crystal is tetragonal (space group *I4/mmm* - D^{17}_{4h}, No. 139); the lattice constants are a = 3.6446 Å and c = 12.2157 Å. The XRD pattern is in agreement with that for undoped $CaGdAlO_4$.

The vibronic properties of an ***a***-cut crystal were studied by Raman spectroscopy, Fig. 1(c). The most intense Raman peak is found at 310 cm^{-1}. It is red-shifted with respect to undoped $CaGdAlO_4$ (330 cm^{-1}) indicating a structure modification. The factor group analysis of the D^{17}_{4h} unit cell predicts the following irreducible representations (***k*** = 0): $\Gamma = 2A_{1g} + 2E_g + 4A_{2u} + 5E_u + B_{2u}$ of which the $2A_{1g}$ and $2E_g$ modes are Raman-active. The band at 310 cm^{-1} is assigned as E_g. The highest phonon frequency $h\nu_{ph}$ is 651 cm^{-1}.

3. Optical spectroscopy

Tm:Ca(Gd,Lu)AlO_4 crystals are optically uniaxial (the optical axis is parallel to the ***c***-axis). There are two principal light polarizations, ***E*** ∥ ***c*** (π) and ***E*** ⊥ ***c*** (σ). All spectroscopic studies were performed using an ***a***-cut crystal at room-temperature (RT, 293 K).

The RT absorption spectra of Tm:Ca(Gd,Lu)AlO_4 for π and σ polarizations are shown in Fig. 2(a). The broad absorption in the visible (300-550 nm) is related to the residual absorption of color centers [25]. The sharp band at 310 nm is due to the Gd^{3+} ions (the $^8S_{7/2} \rightarrow {}^6P_{7/2}$ transition). Note that the $CaLnAlO_4$ crystals have an indirect bandgap E_g of ~4.2 eV [26] corresponding to the UV absorption edge at ~295 nm. In the spectrum, the bands related to Tm^{3+} transitions from the ground-state ($^3H_6$) to the excited ones (from $^3F_4$ up to $^1D_2$) are clearly resolved. The details about the $^3H_6 \rightarrow {}^3H_4$ transition suitable for diode-pumping are shown in Fig. 2(b). The maximum absorption cross-section $\sigma_{abs} = \alpha_{abs}/N_{Tm}$ of 1.66×10^{-20} cm^2 at 792.3 nm corresponds to π-polarization and the full width at half maximum (FWHM) of the

Optics EXPRESS

corresponding absorption peak is 17.5 nm. This is broader than for the 1.8 at.% Tm:CaGdAlO$_4$ crystal studied for comparison (16.3 nm). For σ-polarization, σ_{abs} is 0.67 × 10^{-20} cm^2 at 798.1 nm.

The absorption spectra were analyzed within the standard Judd-Ofelt (J-O) theory [27,28], Table 1. The squared reduced matrix elements for Tm^{3+} ions $U^{(k)}$ were taken from [29]. The J-O (intensity) parameters are Ω_2 = 2.933, Ω_4 = 2.787 and Ω_6 = 1.413 [10^{-20} cm^2].

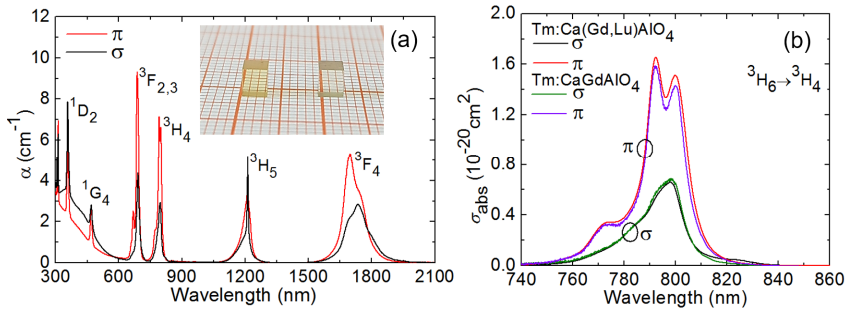

Fig. 2. Absorption of Tm:Ca(Gd,Lu)AlO$_4$: (a) absorption spectrum of the annealed crystal (*α*: absorption coefficient), *inset* – photograph of the sample before (*left*) and after (*right*) annealing; absorption cross-sections, σ_{abs}, for the $^3H_6 \rightarrow {}^3H_4$ Tm^{3+} transition. In (b), the spectra for 1.8 at.% Tm:CaGdAlO$_4$ are also shown. The light polarization is denoted by π and σ.

Table 1. Experimental and Calculated Absorption Oscillator Strengths for Tm:Ca(Gd,Lu)AlO$_4$

Transition	⟨λ⟩, nm	⟨*E*⟩, cm^{-1}	⟨*n*⟩	⟨*Γ*⟩, cm^{-1}nm	$\langle f\rangle_\Sigma^{exp} \times 10^6$	$\langle f\rangle_\Sigma^{calc} \times 10^6$
$^3H_6 \rightarrow {}^3F_4$	1741.8	5741	1.912	407.86	3.523	3.506^{ED}
$^3H_6 \rightarrow {}^3H_5$	1203.4	8310	1.921	131.01	2.371	$2.417^{ED} + 0.527^{MD}$
$^3H_6 \rightarrow {}^3H_4$	794.3	12590	1.933	94.56	3.928	3.656^{ED}
$^3H_6 \rightarrow {}^3F_2 + {}^3F_3$	687.6	14544	1.939	108.58	6.02	5.618^{ED}
$^3H_6 \rightarrow {}^1G_4$	490.7	20378	1.964	14.05	1.529	1.213^{ED}
$^3H_6 \rightarrow {}^1D_2$	362.6	27576	2.009	24.33	4.849	4.685^{ED}
rms deviation						*0.69*

⟨λ⟩ - "center of gravity" of the absorption band, ⟨*E*⟩ - energy barycenter of the multiplet, ⟨*n*⟩ - mean refractive index, ⟨*Γ*⟩ – integrated absorption coefficient, $\langle f\rangle_\Sigma^{exp}$ and $\langle f\rangle_\Sigma^{calc}$ – experimental and calculated absorption oscillator strengths (ED + MD), respectively. The ⟨⟩ brackets indicate polarization-averaging, (2σ + π)/3.

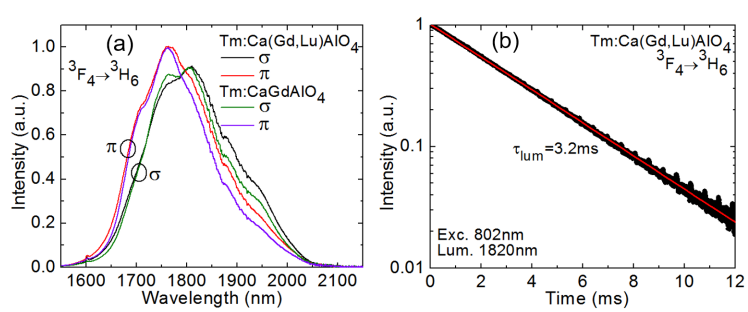

Fig. 3. Luminescence of Tm^{3+} in Ca(Gd,Lu)AlO$_4$: (a) luminescence spectra for the $^3F_4 \rightarrow {}^3H_6$ transition, λ_{exc} = 802 nm; (b) luminescence decay curve, *circles* – experimental data, *line* – single-exponential fit. In (a), the spectra for Tm:CaGdAlO$_4$ are given for comparison. The light polarization is denoted by π and σ.

The polarized luminescence spectra of the Tm:Ca(Gd,Lu)AlO$_4$ crystal (the $^3F_4 \rightarrow {}^3H_6$ Tm^{3+} transition) are shown in Fig. 3(a). The emission spectra are smooth and broad. The highest emission intensity corresponds to π-polarization. The FWHM of the emission

Optics EXPRESS

spectrum is 187 (π) and 207 (σ) nm which is broader than for Tm:$CaGdAlO_4$, 168 (π) and 186 (σ) nm. Thus, the introduction of Lu^{3+} ions leads to an additional spectral broadening due to the compositional disorder.

The luminescence decay of Tm^{3+} ions from the $^3F_4$ multiplet was studied using the pinhole method [30] to diminish the effect of reabsorption on the measured lifetime. The decay curve corresponding to the smallest pinhole (diameter: ~100 μm) is shown in Fig. 3(b). It is clearly single-exponential; the decay time τ_{lum} is 3.2 ms.

The probabilities of spontaneous radiative transitions $A_\Sigma(JJ')$, the luminescence branching ratios $B(JJ')$ and the radiative lifetimes τ_{rad} were calculated using the J-O theory, Table 2. For the upper laser level ($^3F_4$), τ_{rad} = 2.46 ms. This value is shorter than the measured lifetime. The observed difference is attributed to the hypersensitivity of the $^3H_6 \rightarrow {}^3F_4$ transition of Tm^{3+} ions [31] affecting the precision of the J-O calculations. For the $^3H_4$ state, τ_{rad} = 0.44 ms.

Table 2. Calculated Emission Probabilities for Tm^{3+} in Tm:Ca(Gd,Lu)AlO_4

Excited state	Terminal state	⟨λ⟩, nm	$A_\Sigma^{calc}(JJ')$, s^{-1}	$B(JJ')$, %	A_{tot}, s^{-1}	τ_{rad}, ms
$^3F_4$	$^3H_6$	1741.8	407.2^{ED}	100	407.2	2.46
$^3H_5$	$^3F_4$	3893.2	$13.6^{ED} + 1.3^{MD}$	2.5	600.3	1.66
	$^3H_6$	1203.4	$485.6^{ED} + 99.8^{MD}$	97.5		
$^3H_4$	$^3H_5$	2336.5	$58.4^{ED} + 12.2^{MD}$	3.0	2366.8	0.42
	$^3F_4$	1460.2	$182.6^{ED} + 27.8^{MD}$	8.9		
	$^3H_6$	794.3	2085.8^{ED}	88.1		
$^3F_2 + {}^3F_3$	$^3H_4$	5118.8	$7.9^{ED} + 0.2^{MD}$	0.2	5229.4	0.19
	$^3H_5$	1604.2	474.2^{ED}	9.0		
	$^3F_4$	1136.1	$161.8^{ED} + 71.2^{MD}$	4.5		
	$^3H_6$	687.6	4514.1^{ED}	86.3		
$^1G_4$	$^3F_2 + {}^3F_3$	1713.6	$92.8^{ED} + 4.1^{MD}$	2.6	3744.6	0.27
	$^3H_4$	1283.8	$259.4^{ED} + 40.1^{MD}$	8.0		
	$^3H_5$	828.5	$980.7^{ED} + 183.6^{MD}$	31.1		
	$^3F_4$	683.2	$301.1^{ED} + 11.1^{MD}$	8.3		
	$^3H_6$	490.7	1871.7^{ED}	50.0		

⟨λ⟩ - mean emission wavelength estimated from the barycenter energies of multiplets, cf. Table 1, A_Σ^{calc} – probability of radiative spontaneous transitions (ED + MD), $B(JJ')$ – luminescence branching ratio, A_{tot} and τ_{rad} – total probability of radiative spontaneous transitions and radiative lifetime of the excited state, respectively. The $^3F_3 + {}^3F_2$ multiplets are considered as thermally coupled states.

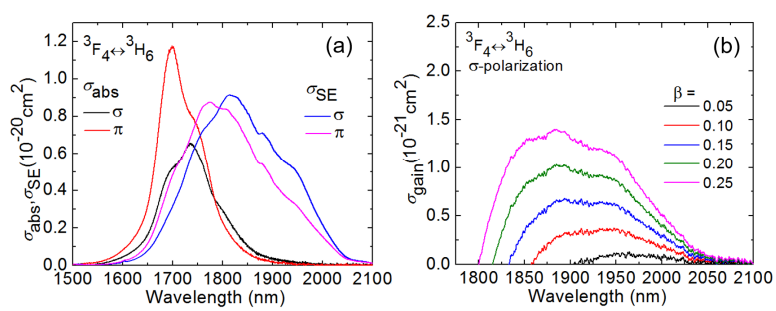

Fig. 4. Transition cross-sections of Tm^{3+} in Ca(Gd,Lu)AlO_4 crystal: (a) absorption, σ_{abs}, and stimulated-emission, σ_{SE}, cross-sections for the $^3F_4 \leftrightarrow {}^3H_6$ transition (π and σ light polarization); (b) gain cross-sections, $\sigma_{gain} = \beta\sigma_{SE} - (1 - \beta)\sigma_{abs}$, for various inversion ratios $\beta = N_2(^3F_4)/N_{Tm}$ (σ light polarization).

The stimulated-emission (SE) cross-sections, σ_{SE}, for the $^3F_4 \rightarrow {}^3H_6$ transition and π and σ polarizations were calculated using a combination of the modified reciprocity method (mRM) [32] and the Füchtbauer–Ladenburg (F-L) equation [33], see Fig. 4(a). The refractive indices were taken from [34], n_o = 1.904 and n_e = 1.927 at ~1.8 μm. The maximum $\sigma_{SE} = 0.91 \times 10^{-20}$ cm^2 at 1813 nm for σ-polarization. As Tm^{3+} ions represent a quasi-three-level laser scheme,

Optics EXPRESS

the laser emission is expected at longer wavelengths. For a local peak in the SE cross-section spectra at 1946 nm for σ-polarization, σ_{SE} is 0.50 × 10^{-20} cm^2.

The gain cross-sections, $\sigma_{gain} = \beta\sigma_{SE} - (1 - \beta)\sigma_{abs}$, where $\beta = N_2(^3F_4)/N_{Tm}$ is the inversion ratio are plotted in Fig. 4(b) for σ-polarization. For small inversion ratios $\beta < 0.10$, the laser emission is expected at ~1950 nm. For $\beta = 0.15$, the gain bandwidth is 145 nm.

4. Laser operation

First, we studied CW operation of Tm:Ca(Gd,Lu)AlO_4 crystal under diode-pumping without any wavelength-selective element in the laser cavity. The active element was ***a***-cut (thickness: t = 3.4 mm, aperture: 3.0(***c***) × 3.0 mm^2). It was polished to laser quality, wrapped with In foil and mounted in a water-cooled (12 °C) Cu-holder providing cooling from all 4 lateral sides. The compact (microchip-type) laser cavity consisted of a plane pump mirror coated for HT at 780-1000 nm and for HR at 1800-2100 nm, and a flat output coupler (OC) having a transmission T_{OC} of 1.5%...20% at the laser wavelength. The pump source was a fiber-coupled (fiber core diameter: 200 µm, N.A. = 0.22) CW AlGaAs laser diode emitting up to 14 W of unpolarized light at 802 nm (FWHM = 3 nm). Its output was collimated and focused into the active element through the PM by a lens assembly (1:1 imaging ratio, focal length f = 30 mm). The radius of the pump beam waist w_P and its Rayleigh length $2z_R$ were 100 µm and 1.73 mm (M^2 ~86), respectively. The pump absorption (double-pass) under lasing conditions was 62%.

The input-output dependences and typical laser emission spectra are shown in Figs. 5(b) and 5(c). The laser output was linearly polarized (σ); the polarization was naturally selected by the gain anisotropy. The maximum output power reached 1.82 W at 1945 nm with a slope efficiency η of 28.4% (with respect to the absorbed pump power P_{abs}) for T_{OC} = 9%. The laser threshold was at P_{abs} = 0.80 W. With the increase of T_{OC}, the emission wavelength blue-shifted from 1955 nm to 1931 nm, Fig. 5(c), in agreement with the gain spectra, Fig. 4(b). We have also studied laser performance of a similar ***c***-cut crystal (t = 3.4 mm). The laser generated 1.22 W at 1944 nm with higher η = 34.4% (for T_{OC} = 9%). The laser emission was unpolarized. The laser operation in the plano-plano cavity indicates positive thermal lens for both ***a***-cut and ***c***-cut crystals.

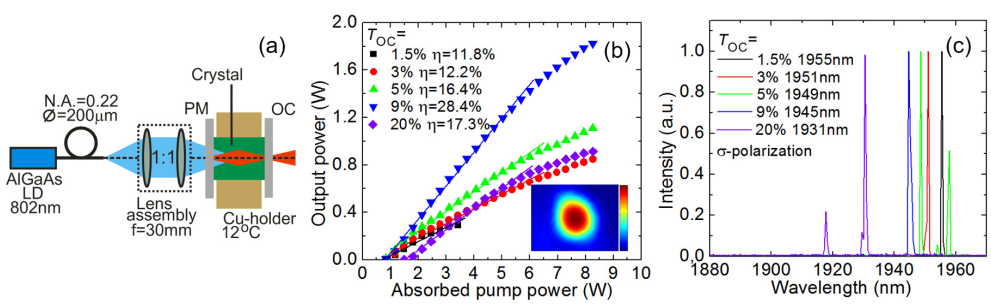

Fig. 5. (a-c) CW diode-pumped Tm:Ca(Gd,Lu)AlO_4 laser: (a) laser set-up: LD – laser diode, PM – pump mirror, OC – output coupler; (a) input-output dependences, η – slope efficiency, *inset* – measured spatial profile of the laser beam for T_{OC} = 9% and maximum P_{abs}; (b) laser emission spectra measured at the maximum P_{abs}. The crystal is ***a***-cut and the laser polarization is σ.

An ***a***-cut 1.8 at.% Tm:CaGdAlO_4 crystal (t = 3.0 mm) was inserted in the same laser set-up for comparison yielding 1.16 W at 1944 nm with η = 31.8%. The laser emission was σ-polarized. Thus, the laser performance of Lu^{3+}-codoped crystals is similar to that of Tm:CaGdAlO_4.

The potential of Tm:Ca(Gd,Lu)AlO_4 for ML laser operation was revealed by studying its wavelength tuning performance in an X-shaped laser cavity, Fig. 6(a). The active element (***a***-cut, t = 6.0 mm, aperture: 3.0 × 3.0 mm^2) was antireflection (AR) coated for pump and laser

Optics EXPRESS

wavelength. It was inserted in the cavity at normal incidence between two folding curved mirrors M1 and M2 (radius of curvature, RoC = 100 mm). M3 was a HR mirror and the transmission of the flat broadband OC was 0.5%...10%. The pump source was a CW Ti:Sapphire laser delivering >3 W at 798 nm (σ-polarization in the crystal). The pump was focused by a spherical lens (f = 70 mm) to a spot with w_P = 30 μm. The pump absorption under lasing conditions measured near the laser threshold was 80.5% (single-pass).

Without any wavelength-selective element in the cavity, the free-running laser generated a maximum output power of 1.18 W at 1942 nm with a maximum η of 51.4% for σ-polarization (***a***-cut crystal, T_{OC} = 10%). The laser threshold was at P_{abs} = 0.13 W. This high slope efficiency value indicates the effect of cross-relaxation for adjacent Tm^{3+} ions, $^3H_4 + {}^3H_6 \rightarrow {}^3F_4 + {}^3F_4$, increasing the pump quantum efficiency above unity. Indeed, the Stokes efficiency for this laser η_{St} is 40.8%.

For the wavelength-tuning experiment, a Lyot filter was inserted in the laser cavity near the OC, Fig. 6(a). It was a 3.2-mm-thick quartz plate with the optical axis at 60° to the surface. Using the ***a***-cut Tm:Ca(Gd,Lu)AlO_4 crystal, the laser wavelength was continuously tuned from 1836 to 2083 nm (tuning range Δλ = 247 nm, T_{OC} = 0.5%) and from 1827 to 2071 nm (Δλ = 244 nm, T_{OC} = 1.5%), Fig. 6(b). A similar experiment was also performed for the ***c***-cut crystal resulting in a tuning range from 1814 to 2072 nm (Δλ = 258 nm, T_{OC} = 0.5%). The laser polarization was σ in all cases.

For achieving fs pulses in ML thulium-doped lasers, it is desirable that the Tm^{3+} emission extends above 2 μm avoiding unwanted atmosphere water vapor absorption. This condition is satisfied in the Tm:Ca(Gd,Lu)AlO_4 laser. The introduction of Lu^{3+} ions provided additional broadening of the emission spectra, Fig. 3(a). This effect is confirmed in the tuning curves. Indeed, for the Tm:$CaGdAlO_4$ (***a***-cut), laser spectral tuning was limited to 2065 nm.

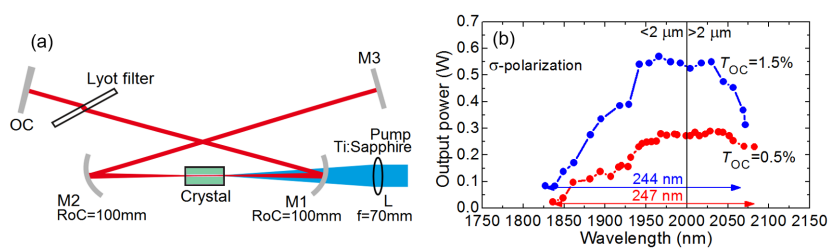

Fig. 6. (a,b) Wavelength tuning of the Tm:Ca(Gd,Lu)AlO_4 laser (***a***-cut crystal): (a) laser set-up: M1 and M2 – folding mirrors, M3 – HR mirror, OC – output coupler, L – lens; (b) wavelength tuning curves (P_{abs} = 2.6 W, laser polarization: σ).

5. Conclusion

To conclude, we report on the growth, structural and spectroscopic characterization, and first CW and wavelength-tunable laser operation of a novel "mixed" disordered calcium aluminate crystal, Tm:Ca(Gd,Lu)AlO_4. The introduction of Lu^{3+} preserves the tetragonal structure and induces additional spectral broadening for the Tm^{3+} absorption and emission bands with respect to Tm:$CaGdAlO_4$. As a consequence, it is attractive for fs ML lasers at ~2 μm. Further work will focus on the codoping of these crystals with Tm^{3+} and Ho^{3+} ions, to shift the emission range further beyond 2 μm (due to the Ho ions), where water vapor absorption has a minor effect on broadband laser generation.

Funding

Spanish Government (MAT2016-75716-C2-1-R (AEI/FEDER,UE) and TEC 2014-55948-R); Generalitat de Catalunya (2017SGR755, 2016FI_B00844, 2017FI_B100158, and 2018 FI_B2 00123); Foundation of President of China Academy of Engineering Physics (YZJJLX2018005); the Government of the Russian Federation (074-U01); and ICREA (2010ICREA-02).

Optics EXPRESS

References

1. J. Petit, P. Goldner, and B. Viana, "Laser emission with low quantum defect in Yb: $CaGdAlO_4$.," Opt. Lett. **30**(11), 1345–1347 (2005).
2. P. O. Petit, J. Petit, P. Goldner, and B. Viana, "Inhomogeneous broadening of optical transitions in Yb:$CaYAlO_4$," Opt. Mater. **30**(7), 1093–1097 (2008).
3. P. Loiko, F. Druon, P. Georges, B. Viana, and K. Yumashev, "Thermo-optic characterization of Yb:$CaGdAlO_4$ laser crystal," Opt. Mater. Express **4**(11), 2241–2249 (2014).
4. Y. Zaouter, J. Didierjean, F. Balembois, G. Lucas Leclin, F. Druon, P. Georges, J. Petit, P. Goldner, and B. Viana, "47-fs diode-pumped Yb^{3+}:$CaGdAlO_4$ laser," Opt. Lett. **31**(1), 119–121 (2006).
5. P. Sévillano, P. Georges, F. Druon, D. Descamps, and E. Cormier, "32-fs Kerr-lens mode-locked Yb:CaGdAlO□ oscillator optically pumped by a bright fiber laser," Opt. Lett. **39**(20), 6001–6004 (2014).
6. F. Druon, M. Olivier, A. Jaffrès, P. Loiseau, N. Aubry, J. DidierJean, F. Balembois, B. Viana, and P. Georges, "Magic mode switching in Yb:$CaGdAlO_4$ laser under high pump power," Opt. Lett. **38**(20), 4138–4141 (2013).
7. R. C. Stoneman and L. Esterowitz, "Efficient, broadly tunable, laser-pumped Tm:YAG and Tm:YSGG cw lasers," Opt. Lett. **15**(9), 486–488 (1990).
8. K. van Dalfsen, S. Aravazhi, C. Grivas, S. M. García-Blanco, and M. Pollnau, "Thulium channel waveguide laser with 1.6 W of output power and ~80% slope efficiency," Opt. Lett. **39**(15), 4380–4383 (2014).
9. J. A. Hutchinson, H. R. Verdun, B. H. Chai, B. Zandi, and L. D. Merkle, "Spectroscopic evaluation of $CaYAlO_4$ doped with trivalent Er, Tm, Yb and Ho for eyesafe laser applications," Opt. Mater. **3**(4), 287–306 (1994).
10. R. Moncorgé, N. Garnier, P. Kerbrat, C. Wyon, and C. Borel, "Spectroscopic investigation and two-micron laser performance of Tm^{3+}:$CaYAlO_4$ single crystals," Opt. Commun. **141**(1–2), 29–34 (1997).
11. W. Wang, X. Yan, X. Wu, Z. Zhang, B. Hu, and J. Zhou, "Study of single-crystal growth of Tm^{3+}:$CaYAlO_4$ by the floating-zone method," J. Cryst. Growth **219**(1–2), 56–60 (2000).
12. Z. P. Qin, J. G. Liu, G. Q. Xie, J. Ma, W. L. Gao, L. J. Qian, P. Yuan, X. D. Xu, J. Xu, and D. H. Zhou, "Spectroscopic characteristics and laser performance of Tm:$CaYAlO_4$ crystal," Laser Phys. **23**(10), 105806 (2013).
13. J. Di, X. Xu, C. Xia, Q. Sai, D. Zhou, Z. Lv, and J. Xu, "Growth and spectra properties of Tm, Ho doped and Tm, Ho co-doped $CaGdAlO_4$ crystals," J. Lumin. **155**, 101–107 (2014).
14. J. Lan, B. Xu, Z. Zhou, H. Xu, Z. Cai, X. Xu, J. Xu, and R. Moncorgé, "High-power CW and Q-switched Tm:$CaYAlO_4$ lasers at 1.94 µm for shallow water absorption," IEEE Photonics Technol. Lett. **29**(23), 2127–2130 (2017).
15. J. Lan, Z. Zhou, X. Guan, B. Xu, H. Xu, Z. Cai, X. Xu, D. Li, and J. Xu, "Passively Q-switched Tm:$CaGdAlO_4$ laser using a Cr^{2+}:ZnSe saturable absorber," Opt. Mater. Express **7**(6), 1725–1731 (2017).
16. W. Yao, F. Wu, Y. Zhao, H. Chen, X. Xu, and D. Shen, "Highly efficient Tm:CaYAlO₄ laser in-band pumped by a Raman fiber laser at 1.7 µm," Appl. Opt. **55**(14), 3730–3733 (2016).
17. Y. Wang, G. Xie, X. Xu, J. Di, Z. Qin, S. Suomalainen, M. Guina, A. Härkönen, A. Agnesi, U. Griebner, X. Mateos, P. Loiko, and V. Petrov, "SESAM mode-locked Tm:CALGO laser at 2 µm," Opt. Mater. Express **6**(1), 131–136 (2016).
18. L. C. Kong, Z. P. Qin, G. Q. Xie, X. D. Xu, J. Xu, P. Yuan, and L. J. Qian, "Dual-wavelength synchronous operation of a mode-locked 2-µm Tm:$CaYAlO_4$ laser," Opt. Lett. **40**(3), 356–358 (2015).
19. P. Loiko, X. Mateos, S. Y. Choi, F. Rotermund, J. M. Serres, M. Aguiló, F. Díaz, K. Yumashev, U. Griebner, and V. Petrov, "Vibronic thulium laser at 2131 nm Q-switched by single-walled carbon nanotubes," J. Opt. Soc. Am. B **33**(11), D19–D27 (2016).
20. A. Schmidt, P. Koopmann, G. Huber, P. Fuhrberg, S. Y. Choi, D.-I. Yeom, F. Rotermund, V. Petrov, and U. Griebner, "175 fs Tm:Lu_2O_3 laser at 2.07 µm mode-locked using single-walled carbon nanotubes," Opt. Express **20**(5), 5313–5318 (2012).
21. Y. Wang, W. Chen, M. Mero, L. Zhang, H. Lin, Z. Lin, G. Zhang, F. Rotermund, Y. J. Cho, P. Loiko, X. Mateos, U. Griebner, and V. Petrov, "Sub-100 fs Tm:$MgWO_4$ laser at 2017 nm mode locked by a graphene saturable absorber," Opt. Lett. **42**(16), 3076–3079 (2017).
22. Y. Wang, W. Jing, P. Loiko, Y. Zhao, H. Huang, X. Mateos, S. Suomalainen, A. Härkönen, M. Guina, U. Griebner, and V. Petrov, "Sub-10 optical-cycle passively mode-locked Tm:$(Lu_{2/3}Sc_{1/3})_2O_3$ ceramic laser at 2 µm," Opt. Express **26**(8), 10299–10304 (2018).
23. Y. Wang, Y. Zhao, Z. Pan, J. E. Bae, S. Y. Choi, F. Rotermund, P. Loiko, J. M. Serres, X. Mateos, H. Yu, H. Zhang, M. Mero, U. Griebner, and V. Petrov, "78 fs SWCNT-SA mode-locked Tm:CLNGG disordered garnet crystal laser at 2017 nm," Opt. Lett. **43**(17), 4268–4271 (2018).
24. Q. Hu, Z. Jia, A. Volpi, S. Veronesi, M. Tonelli, and X. Tao, "Crystal growth and spectral broadening of a promising Yb:$CaLu_xGd_{1-x}AlO_4$ disordered crystal for ultrafast laser application," CrystEngComm **19**(12), 1643–1647 (2017).
25. A. Jaffres, S. K. Sharma, P. Loiseau, B. Viana, J. L. Doualan, and R. Moncorgé, "UV-visible luminescence properties of the broad-band Yb:CALGO laser crystal," in *Advanced Solid State Lasers* (Optical Society of America, 2014), p. ATu2A.9.
26. R. V. Perrella, C. N. Júnior, M. S. Goes, E. Pecoraro, M. A. Schiavon, C. O. Paiva-Santos, H. Lima, M. A. Couto dos Santos, S. J. L. Ribeiro, and J. L. Ferrari, "Structural, electronic and photoluminescence properties of Eu^{3+}-doped $CaYAlO_4$ obtained by using citric acid complexes as precursors," Opt. Mater. **57**, 45–55 (2016).

Optics EXPRESS

27. B. R. Judd, "Optical absorption intensities of rare-earth ions," Phys. Rev. **127**(3), 750–761 (1962).
28. G. S. Ofelt, "Intensities of crystal spectra of rare-earth ions," J. Chem. Phys. **37**(3), 511–520 (1962).
29. B. M. Walsh, N. P. Barnes, and B. Di Bartolo, "Branching ratios, cross sections, and radiative lifetimes of rare earth ions in solids: Application to Tm^{3+} and Ho^{3+} ions in $LiYF_4$," J. Appl. Phys. **83**(5), 2772–2787 (1998).
30. H. Kühn, S. T. Fredrich-Thornton, C. Kränkel, R. Peters, and K. Petermann, "Model for the calculation of radiation trapping and description of the pinhole method," Opt. Lett. **32**(13), 1908–1910 (2007).
31. P. A. Ryabochkina, S. A. Antoshkina, E. V. Bolshakova, M. A. Ivanov, V. V. Kochurihin, A. V. Malov, S. N. Ushakov, N. V. Shchuchkina, and K. N. Nishchev, "K.N., "Hypersensitive transitions of Tm^{3+}, Ho^{3+} and Dy^{3+} rare-earth ions in garnet crystals," J. Lumin. **132**(8), 1900–1905 (2012).
32. A. S. Yasyukevich, V. G. Shcherbitskii, V. E. Kisel', A. V. Mandrik, and N. V. Kuleshov, "Integral method of reciprocity in the spectroscopy of laser crystals with impurity centers," J. Appl. Spectrosc. **71**(2), 202–208 (2004).
33. B. Aull and H. Jenssen, "Vibronic interactions in Nd:YAG resulting in nonreciprocity of absorption and stimulated emission cross sections," IEEE J. Quantum Electron. **18**(5), 925–930 (1982).
34. P. Loiko, P. Becker, L. Bohatý, C. Liebald, M. Peltz, S. Vernay, D. Rytz, J. M. Serres, X. Mateos, Y. Wang, X. Xu, J. Xu, A. Major, A. Baranov, U. Griebner, and V. Petrov, "Sellmeier equations, group velocity dispersion, and thermo-optic dispersion formulas for CaLnAlO₄ (Ln = Y, Gd) laser host crystals," Opt. Lett. **42**(12), 2275–2278 (2017).